Carcinogenesis vol.35 no.7 pp.1661–1670, 2014
doi:10.1093/carcin/bgu090
Advance Access publication April 17, 2014

Endothelial cell-derived fibronectin extra domain A promotes colorectal cancer metastasis via inducing epithelial–mesenchymal transition

Juanjuan Ou[†], Yuan Peng[†], Jia Deng, Hongming Miao, Jie Zhou, Lin Zha, Rongbin Zhou, Liqing Yu,[1] Hang Shi[2] and Houjie Liang*

Department of Oncology and Southwest Cancer Center, Southwest Hospital, Third Military Medical University, Chongqing 400038, China, [1]Department of Animal and Avian Sciences, University of Maryland, College Park, MD 20742, USA and [2]Department of Biology, Georgia State University, Atlanta, GA 30303, USA

*To whom correspondence should be addressed. Tel: 86-23-68754128; Fax: 86-23-65425219;
Email: lianghoujie@sina.com

Recent evidence has been suggesting the important roles of endothelial cells (ECs) involved in the pathogenesis of several cancers, including colorectal carcinomas (CRCs), but the underlying mechanism remains elusive. We have demonstrated previously that CRC-derived fibronectin extra domain A (EDA) promotes vasculogenesis, tumorigenesis and metastasis of CRCs. At the current study, we showed that EC-secreted EDA promotes the metastatic capacity CRC cells via inducing an epithelial–mesenchymal transition. *In vitro* and *in vivo* experiments showed that EC-secreted EDA, via the interaction with integrin α9β1 on neighboring CRC cells, leads to the activation of focal adhesion kinase as well as Rac signalings, thus strengthens the polarity of cytoskeleton and promotes the invasion capacity of CRC cells. Furthermore, Erk signaling pathway was revealed to critically mediate the effect of EC-derived EDA on CRC cells. Our findings reveal a novel oncogenic role of ECs in promoting CRC malignancy through secreting EDA.

Introduction

It is well demonstrated that cancer cells critically contribute to tumor vasculogenesis (1,2), and abundant neovascularization is a hallmark of highly aggressive malignant tumors, including colorectal carcinomas (CRCs) (3). Although tumor vascularity correlates with the invasion capacity of CRCs, this does not necessarily just imply an associated increase in blood supply (4,5). It is possible that endothelial cell (EC) plays a more active role in regulating tumor cell behaviors than simply providing the physical structure that forms conduits for blood flow. The observation that cancer stem cells (CSCs) accumulate in perivascular regions has been reported by several groups (6,7), and EC-secreted factors have been shown to promote the characteristics of CSCs in several kinds of cancers (7–9). These studies strongly suggest that tumor-associated EC plays a critical role in promoting tumor malignancies, but the underlying mechanism is largely unrevealed.

Tumor microenvironment has been reported to play important roles in promoting cancer pathogenesis. We and others have shown previously that an important component of tumor microenvironment, alternative extra domain A (EDA) of fibronectin, promotes vasculogenesis, tumorigenesis and metastasis of colorectal tumors (10–15). It has also been reported that EDA is a vascular marker of solid tumors (10); however, studies on the role of EC-derived EDA in tumor malignancy have not been reported. Very importantly and impressively, we found that in CRCs, ECs also express and secret abundant EDA and that EDA receptor, integrin α9β1-positive CRC cells, mainly resides in the perivascular niches. Integrin α9β1 is a specific receptor for EDA (16), and it was recently implicated in promotion of tumor cell invasion in breast cancer (17). Collectively, these findings led us to the hypothesis that EC-derived EDA plays a pivotal role in promoting CRC metastasis via interacting with integrin α9β1 on neighboring CRC cells. The purpose of this study was to investigate the role of EC-derived EDA in CRC metastasis and the underlying mechanism by which this occurs.

Abbreviations: CRC, colorectal carcinoma; CSC, cancer stem cell; EC, endothelial cell; EDA, extra domain A of fibronectin; ERK, extracellular signal-regulated kinase; EMT, epithelial–mesenchymal transition; FAK, focal adhesion kinase; FBS, fetal bovine serum; hCRC, human CRC cell; HUVEC, human umbilical vein EC; IgG, immunoglobulin G; mRNA, messenger RNA; shRNA, short hairpin RNA.

[†]These authors contributed equally to this work.

Materials and methods

Tissue samples

A total of 200 tissue specimens used for primary cell isolation, immunohistochemistry, immunofluorescence microscopy and western blot studies were collected from CRC patients who had undergone surgeries at Southwest Hospital, the Third Military Medical University. Tumors were staged by anatomic pathologists in the Department of Pathology, Southwest Hospital, according to the Union for International Cancer Control classification system. Half of each fresh tissue sample was used for primary cell isolation, a piece of each specimen was snap-frozen in liquid nitrogen, then stored at −70°C ultrafreezers for immunofluorescence staining, messenger RNA (mRNA) and protein isolation, and the rest was fixed in 10% formaldehyde and embedded in paraffin for histological sections. All human experiments were approved by the Ethics Committee of Southwest Hospital, the Third Military Medical University.

Cell culture

The human colon cancer cell lines, HCT116 and HT-29, and human fibroblast cell line BJ were obtained from the American Type Culture Collection (ATCC, Manassas, VA) and maintained in McCoy's 5A or Dulbecco's modified Eagle's medium (Invitrogen Corp.) supplemented with 10% fetal bovine serum (FBS) at 37°C under 5% CO_2. The human umbilical vein ECs (HUVEC)-C line purchased from ATCC was maintained in ATCC formulation of F-12K Medium (Cat# 30-2004) with the following components, 0.1 mg/ml heparin; 0.03–0.05 mg/ml EC growth supplement, and supplemented with FBS at 37°C under 5% CO_2. Freshly isolated CRC cells were maintained in Dulbecco's modified Eagle's medium (Invitrogen Corp.) supplemented with 10% FBS at 37°C under 5% CO_2, and freshly isolated ECs were cultured in ATCC formulation of F-12K Medium with 0.1 mg/ml heparin, 0.03–0.05 mg/ml EC growth supplement, supplemented with FBS at 37°C under 5% CO_2.

Antibodies and reagents

A monoclonal anti-focal adhesion kinase (FAK) antibody was obtained from Upstate Biotechnology (Upstate, Waltham, MA). A polyclonal anti-phospho-FAK (phospho-Tyr397) antibody and anti-phospho-c-Src (Y416) were purchased from BD Biosciences (San Diego, CA). A rabbit monoclonal anti-phospho-Akt, a rabbit polyclonal anti-Akt antibody, a rabbit monoclonal anti-phospho-p44/42 mitogen-activated protein kinase (Erk1/2) and a mouse monoclonal anti-Erk antibody were from Cell Signaling (Beverly, MA). Mouse monoclonal antibodies against human fibronectin EDA domain (IST-9), integrins α4β1 and α4β7, integrin α9β1 and isotype control antibody [mouse immunoglobulin G1 (IgG1)] for these antibodies were purchased from Abcam. Monoclonal anti-E-cadherin was purchased from Epitomics. Epithelial–Mesenchymal Transition (EMT) Antibody Sampler Kit and a monoclonal anti-glyceraldehyde 3-phosphate dehydrogenase antibody for western blotting were purchased from Cell Signaling. A monoclonal antibody of anti-c-Src was from Santa Cruz Biotechnology (Santa Cruz, CA). A mouse monoclonal antibody against integrin β1 was purchased from Chemicon (Temecula, CA). Phalloidin (TRITC) was purchased from Sigma. Recombinant transforming growth factor β was obtained from R&D System.

Immunohistochemical and immunofluorescence microscopy studies

All tissue chip slides were routinely dewaxed, rehydrated and prepared for immunohistochemistry. The slides were incubated in 0.3% H_2O_2 in methanol for 30 min to block endogenous peroxidase. Antigens were retrieved with 10 mmol/l sodium citrate (pH 6) for 15 min in a microwave oven. The slides were then incubated with the selected antibody at 37°C for 1 h and at 4°C overnight. Slides without treatment with the primary antibody served as

negative controls. The slides were developed with an EnVisionTM method (DAKO, Capinteria, CA). The slides were visualized using the diaminobenzidine solution (DAKO) and then lightly counterstained with hematoxylin. Immunohistochemical staining was scored from 0 to 4 as follows. No staining = 0; weak staining = 1; strong staining of 25% or moderate staining of <80% tumor cells = 2; strong staining of 25–50% or moderate staining of >80% tumor cells = 3; strong staining of >50% tumor cells = 4. Meanwhile, score 0–1 as negative (recorded as −) and 2–4 as positive (2 recorded as +, 3 as ++, 4 as +++). Ten representative areas were counted from high power fields for each tissue section. Slides were examined and scored independently by three pathologists blinded to other patient information.

Frozen tissue samples for immunofluorescence staining were cut into 4 μm serial sections. All the frozen sections were fixed in ice-acetone for 20 min, washed with phosphate-buffered saline for three times for 5 min each and incubated for 30 min at room temperature in a protein-blocking solution. The sections were incubated with the primary antibodies for 1 h at 37°C and then at 4°C overnight. After wash, the sections were incubated at 37°C for 1 h with appropriate secondary antibodies, including fluorescein isothiocyanate-conjugated goat anti-rabbit IgG (1:50, Santa Cruz Biotechnology), fluorescein isothiocyanate-conjugated goat anti-mouse IgG (1:50, Santa Cruz Biotechnology) or TRITC-conjugated goat anti-mouse IgG (1:50, Beyotime, China). The sections were counterstained with Hoechst 33258 to reveal cell nuclei.

Clonogenic assay

For clonogenic assays, cells were plated into 24 well plates. Ten days later after plating, colonies were stained using the crystal violet solution and the number of epithelial cells, scattered cells and highly scattered cells were calculated using ImageJ software.

FAK and Rac1 knockdown plasmids and establishment of stable cell lines

FAK short hairpin RNA (shRNA) and control plasmids were obtained and used as described previously (18). Rac1 siRNA and control plasmids were purchased from Santa Cruz Biotechnology. All resultant constructs were verified by DNA sequencing and then transfected into target cells with lipofectamine™ 2000 transfection reagent (Invitrogen, Carlsbad, CA). Transfected cells were enriched by selection for 1 week with antibiotics selection.

Lentiviral particles and establishment of stable cell lines

The lentiviral particles for EDA overexpression and knockdown were purchased from GeneChem Co., Ltd (Shanghai, China). Stably transfected cells were established following the manufacturer's instructions as we described previously (14) and the detail information for EDA expression and silence vector system was included in Supplementary Materials, available at *Carcinogenesis* Online.

Protein extraction and western blotting

Cell lysates were prepared with M-PER Mammalian Protein Extraction Reagent (Pierce, Rockford, IL). A total of 30 μg of lysate proteins were separated by sodium dodecyl sulfate–polyacrylamide gel electrophoresis after heat denature, transferred onto polyvinylidene difluoride membranes and incubated with 5% non-fat milk dissolved in phosphate-buffered saline–Tween 20 solution for 1 h, followed by incubation with a primary antibody overnight at 4°C. After wash, the membranes were incubated with an appropriate horseradish peroxidase-conjugated secondary antibody and then developed with enhanced chemiluminescence detection reagents (Amersham Pharmacia Biosciences).

Coimmunoprecipitation assay

Total protein lysates (500 μg) from each sample were immunoprecipitated in 400 μl lysate buffer containing 2 μl anti-EDA mouse monoclonal antibody and inhibitors of various proteases, phosphotases and kinases at 4°C for 4 h with rotation. Protein A-conjugated agarose beads (25 μl) were then added into the immunoprecipitation reaction with an additional 5 h of rotation at 4°C. The antigen–antibody complexes were precipitated by a quick centrifugation, followed by four times of wash with cold phosphate-buffered saline. Controls included an aliquot of rabbit serum to replace the EDA antibody in the immunoprecipitation reaction. The pellets were suspended in 20 μl of 2× sodium dodecyl sulfate reducing western blot loading buffer and boiled for 10 min, followed by sodium dodecyl sulfate–polyacrylamide gel electrophoresis. The EDA immunoprecipitates were subjected to western blot assay to detect EDA and integrin α9β1 in the immunoprecipitates. Rac1 activity assay was measured as described in ref. (19).

Enzyme-linked immunosorbent assay

EDA concentrations in the sera of patients with CRC were quantified using a human fibronectin EDA-specific enzyme-linked immunosorbent assay kit (BPE301106H, RB, Shanghai Hushang Biotechnology Co., Ltd).

Quantitative real-time PCR

Total RNAs were isolated using a Peqgold Total RNA Kit including DNase digestion (Peqlab, Erlangen, Germany). RNAs were transcribed into complementary DNAs using Omniscript (Qiagen, Hilden, Germany). Quantitative real-time PCR was performed using the 7900HT Fast Real-Time PCR system (Applied Biosystems, Darmstadt, Germany). Expression levels were normalized to β-actin. Reactions were done in duplicate using Applied Biosystems Taqman Gene Expression Assays and Universal PCR Master Mix. The relative expression was calculated by the $2^{(-DDCt)}$ method. The primers are available upon request.

Transwell assay

The migration ability of cells was assessed using transwell chambers with polycarbonate membrane filters with 24 well inserts (6.5 mm diameter and 8 μm pore size) (Corning Life Sciences, Corning, NY). The membrane filters were coated with 1.5 mg/ml Matrigel™ (BD Biosciences, Franklin Lakes, NJ) before use. A total of 5000 cells in 150 μl of McCoy's 5A Modified Medium with antibiotics but without serum were seeded into the upper chamber. The lower chamber was filled with 600 μl McCoy's 5A Modified Medium supplemented with antibiotics and 30% FBS. The medium in both chambers was changed once daily. After culture for 48 h, following removal of the non-migratory cells from the upper surface of the filter using a Q-tip, the migrated cells were fixed with cooled acetone (4°C) and then stained with crystal violet solution (Invitrogen) and counted under 10 different low-power (×100) microscopic fields. The cell border was verified by switching to the high-power objective lens (×400) during counting.

In vivo *tumor models*

Four- to six-week-old Balb/c nude mice (body weight: 16–20 g) were purchased from the Experimental Animal Center, Institute of Laboratory Animal Sciences, China, and maintained in a specific pathogen-free environment in accordance with the National Institutes of Health guidelines (Guide for the Care and Use of Laboratory Animals, 1996). The mice were subcapsularly injected with cancer cells into the spleens. For metastatic capacity determination, the mice were killed 6 weeks after injection and the xenografts were collected. A half of a xenograft was fixed in 4% formalin and embedded in paraffin blocks, and the remainder was snap-frozen in liquid nitrogen for histological studies. Livers and lungs were collected for preparing paraffin and frozen sections at 8 μm. For survival determination, animals were dissected after death. All of our animal studies have been approved by the Institutional Animal Care and Use Committee of the Third Military Medical University.

Statistical analysis

Data are expressed as mean ± SEM. The pathologic scoring data of human specimens were analyzed by two biostatisticians in the Department of Statistics, the Third Military Medical University, China. The statistical analysis was performed by one-way analysis of variance (when >3 groups) or Student's *t*-test (between two groups) using Graph Pad Prism software. For cancer survival analysis, Kaplan–Meier survival curves of overall survival were used. For the analysis of correlation between EDA and integrin expression levels and clinical parameters, or between EDA and integrin expression levels in CRC patients with recurrence and EDA and integrin expression levels in CRC patients without recurrence, Fisher's exact test was used. For the correlation analysis of expression levels between EDA and integrin and other proteins in human tissues, non-parametric Mann–Whitney *U*-test was performed and Spearman's rho was calculated using SPSS 17.0 software. Differences between the values were considered statistically significant when $P < 0.05$.

Results

EC-secreted EDA promotes the invasion capacity of CRC cells

We and others have showed that CRC cell-derived EDA promotes tumor vasculogenesis and metastasis (10–15). Intriguingly, we found that ECs also expressed abundant EDA (Figure 1A), and EC-secreted EDA could be detected in the culture medium of freshly isolated human microvessel endothelial cells from human CRCs (Figure 1B). More impressively, secreted EDA level of human microvessel endothelial cells from patients of advanced stages was significantly higher than that from patients of early stages (Figure 1B), indicating that EC-derived EDA was involved in CRC pathogenesis. Given the important role of tumor cell-derived EDA reported in the previous studies, we sought to unequivocally clarify the relative contribution of different cells to EDA pool in CRC microenvironment. Based on the same amount of cell protein, we unexpectedly found that (i) secreted

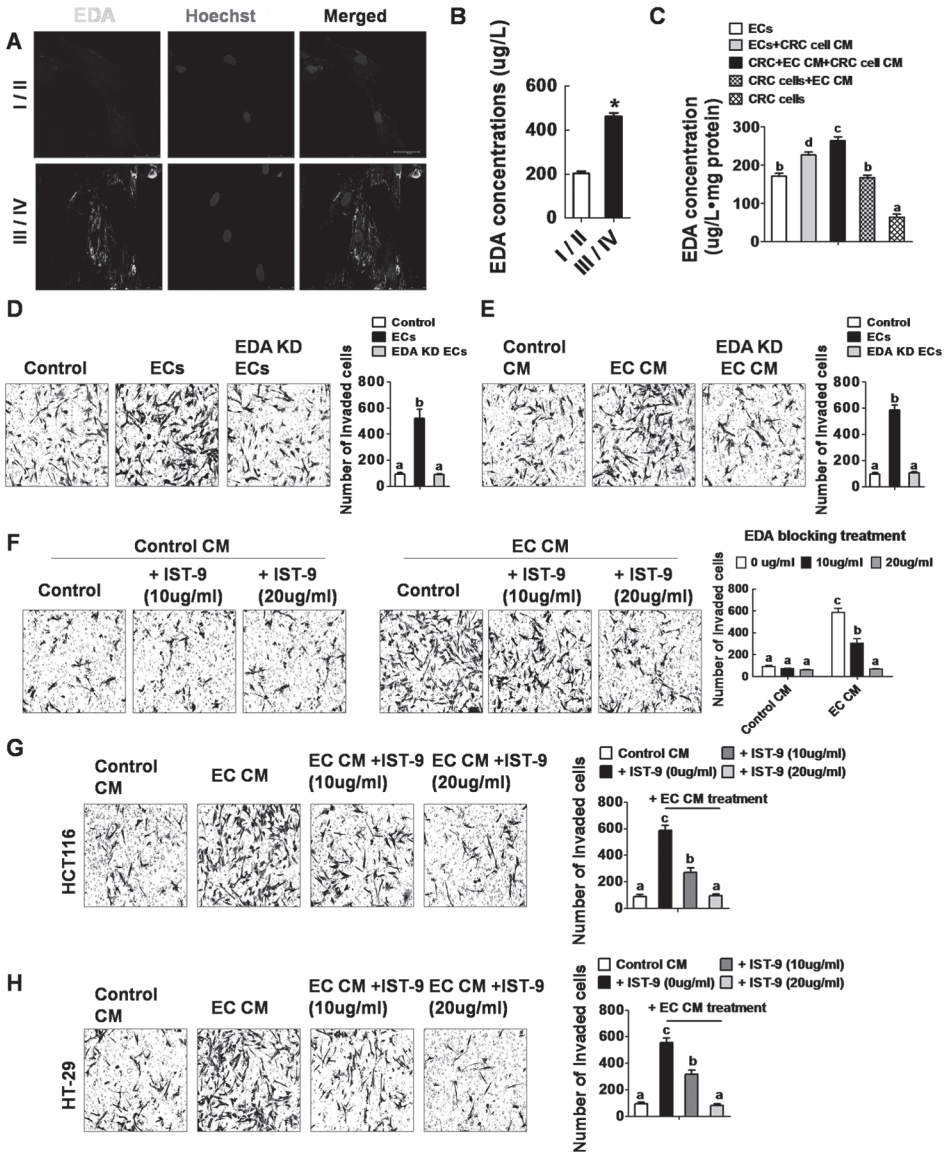

Fig. 1. EC-derived EDA promotes the invasion capacity of CRC cells. (**A**) Immunofluorescent staining of EDA in primary ECs isolated from the CRC tumors of different stages. (**B**) The secreted EDA concentrations in the culture medium of primary ECs isolated from patients with different stages. $n = 32$ for stages I/ II. $n = 45$ for stages III/IV. *$P < 0.01$. (**C**) The secreted EDA concentrations in the culture medium of different combination of CRC cells and ECs. (**D**) Transwell assays of the invasion ability of primary CRC cells cultured in normal medium or cocultured with control ECs or EDA knockdown (KD) ECs. (**E**) Transwell assays of the invasion ability of primary CRC cells cultured in normal medium or conditional culture medium (CM) from control ECs and EDA KD ECs. (**F**) Transwell assays of the invasion ability of control or EC CM-pretreated primary CRC cells in the presence of different dose of EDA antibody (IST-9) treatment. (**G** and **H**) Transwell assays of the invasion ability of EC CM-pretreated colon cancer cell line HCT116 and HT-29 cells in the presence of different dose of EDA antibody (IST-9) treatment. Statistical analysis was done using one-way analysis of variance, and different letters associated with individual bars represent significant statistical differences among the groups ($P < 0.01$).

EDA level of single cultured EC group was significantly higher than that of single cultured CRC cell group; (ii) secreted EDA level of ECs treated with CRC cell CM was modestly higher than that of single cultured ECs; (iii) secreted EDA level of CRC cells treated with EC CM got a sharp increase relative to that of single-cultured-CRC cells; (iv) CRC cells treated with CRC cell CM plus EC CM showed the highest secreted EDA level compared with those in the other groups (Figure 1C). All these data suggest that EC-derived EDA critically contributes to the EDA pool in CRC microenvironment.

To investigate the potential effect of EC-derived EDA on CRC cells, we first conducted a coculture experiment. We used freshly isolated human CRC cells (hCRCs) and freshly isolated HUVECs. After coculture in transwell system for 2 days, we found that HUVECs significantly facilitated the invasion capacity of cocultured CRC cells (Figure 1C), whereas intriguingly, EDA-silenced HUVECs failed to facilitate under the same condition (Figure 1D). To further identify whether this effect required cell–cell crosstalk or was just induced by soluble EDA secreted by ECs, we supplied CRC cells with conditioned medium (CM) obtained from freshly isolated HUVECs, EDA-silenced HUVECs or control medium (Dulbecco's modified Eagle's medium containing 1% FBS). After exposure to the CM for 24 h, CRC cells were analyzed for invasion capacity. Compared with control medium, HUVEC CM dramatically promoted the invasion of hCRC cells by 6-fold in comparison with control CM, whereas CM of EDA-silenced HUVECs showed similar effect on CRC cell invasion as control CM (Figure 1E). Additionally, the increased invasion of CRC cells induced by HUVEC CM could be reversed by EDA antibody treatment in a dose-dependent manner (Figure 1F). We were able to obtain similar results from established CRC cell lines (HCT116 and HT29) treated with CM collected from established HUVEC-C

line (Figure 1G and H). Taken together, these data demonstrate that EC-secreted EDA significantly promotes CRC cell invasion *in vitro*. For all the subsequent experiments, CM from ECs from human CRCs has been used.

EC-derived EDA induces EMT in CRC cells

Strikingly, like the phenotype induced by transforming growth factor β, EC CM-treated CRC cells were found to acquire fibroblast-like morphology and were loosely scattered (Figure 2A), and the highly scattered cells in EC CM-treated hCRC cells were significantly more than those in control group (Figure 2B). These data strongly suggest that an EMT of cocultured CRC cells was induced by EC CM treatment. We then sought to measure the shifts of EMT markers, and expectedly, the mRNA and protein level of E-cadherin, an epithelial marker, dramatically decreased, whereas the levels of mesenchymal markers, Snail and vimentin significantly increased in EC CM-treated CRC cells (Figure 2C and D). Furthermore, the induced EMT of CRC cells by EC CM treatment could be reversed by EDA-blocking treatment (Figure 2E and F). As important controls, CM obtained from freshly isolated human CRC cells, established CRC cell lines (HCT116 and HT29) or fibroblast cell line (BJ) was not able to induce EMT phenotype in treated CRC cells (Figure 2G). A critical experiment for determining the EMT phenotype is the *in vivo* metastasis potential (20). We therefore sought to validate our *in vitro* findings by using an *in vivo* model. To this end, CRC cells pretreated with EC CM, EDA-silenced EC CM or control CM were used to establish a splenic injection model to induce liver metastasis, the most common site of CRC metastasis (20). Although no significant difference was found between the group of treated with control medium and the group of treated with EDA-silenced EC CM, CRC cells treated with EC CM showed a significantly increased incidence of liver metastasis (9 of 10 in EC CM group, 1 of 10 in EDA-silenced EC CM group and

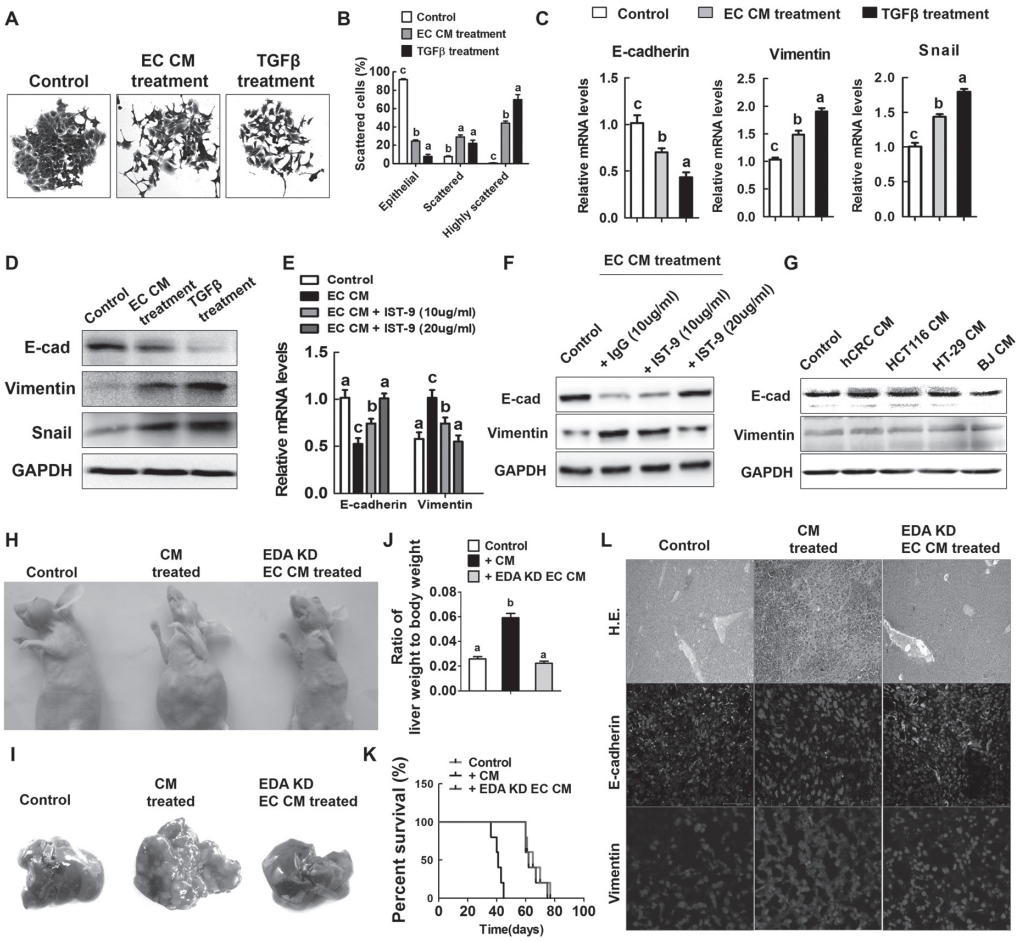

Fig. 2. EC CM treatment induces an EMT in CRC cells. (**A**) Morphology of control and EC CM-treated primary human CRC cells in colony culture condition. (**B**) For statistical analysis of scattered cells, 100 cells in each colony were counted under microscopy (×200). A total of 10 colonies were counted for each group. The cells attached to each other tightly were considered as 'Epithelial'. The cells scattered, but still attached to other cells were considered 'Scattered'. The scattered cells that had no contact with other cells were considered 'Highly scattered'. Statistical analysis was done using one-way analysis of variance (ANOVA), and different letters associated with individual bars represent significant statistical differences among the groups ($P < 0.01$). (**C** and **D**) Real-time PCR and western blots of the EMT marker expressions in EC CM-treated and control primary human CRC cells compared with that in transforming growth factor β (5 ng/ml)-treated group. (**E** and **F**) Real-time PCR and western blots of EMT marker expressions in control or EC CM-pretreated primary human CRC cells in the presence of different dose of EDA-blocking (IST-9) treatment. Statistical analysis was done using one-way ANOVA, and different letters associated with individual bars represent significant statistical differences among the groups ($P < 0.01$). (**G**) Western blots of EMT marker expressions of control or CM-treated primary human CRC cells (CM from primary CRC cells, colon cancer cell line HCT116 cells, colon cancer cell line HT-29 cells or fibroblast cell line BJ). (**H**) Macroscopic appearance of the mice subcapsularly injected with control, EC CM-treated and EDA knockdown (KD) EC CM-treated primary human CRC cells into the spleens at 40 days of age. (**I**) A photograph of a representative liver in each group is also shown. (**J**) Statistical analysis of the ratio of liver weight to body weight. Statistical analysis was done using one-way ANOVA, and different letters associated with individual bars represent significant statistical differences among the groups ($P < 0.001$; $n = 9$ in each group in all experiments). (**K**) Statistical analysis of the overall survival of the mice subcapsularly injected with control, EC CM-treated and EDA KD EC CM-treated primary CRC cells into the spleens ($n = 9$ in each group). $P < 0.01$ (Kaplan–Meier survival curves). (**L**) Representative hematoxylin and eosin sections of the liver, immunofluorescence staining of E-cadherin and vimentin of a representative xenograft in each group is also shown.

2 of 10 in the control group) and a substantially increased tumor burden 6 weeks after injection, as demonstrated by an significant increase of the ratio of liver weight to bodyweight (Figure 2H–J). Expectedly, the nude mice with the xenograft generated by EC CM-pretreated CRC cells showed a dramatically shorter survival (Figure 2K). To further confirm the EMT phenotype of injected CRC cells induced by EC CM, we immunostained the xenografts with EMT marker antibodies, and the results demonstrated that the expression level of E-cadherin dramatically decreased, whereas the level of vimentin increased in the xenografts of EC CM-treated group in comparison with those of control group and the group treated with EDA-silenced EC CM (Figure 2L). Collectively, these data support our hypothesis that EC-derived EDA promotes the metastatic potential of CRCs, at least in part, via inducing EMT of CRC cells.

Integrin α9β1 is critically required for the effect of EC-secreted EDA on CRC cells

The effect exhibited by EC-secreted EDA on CRC cells suggests the existence of a cell surface receptor that mediates this interaction. In an attempt to identify such a receptor, we first determined CRC cell invasion induced by EC-derived EDA in the presence of blocking antibodies for integrins α4β1, α4β7 and α9β1, which are known to bind EDA segment (21). Impressively, blocking of integrin α9β1 reversed the EC CM-induced invasion of CRC cells (Figure 3A), whereas blocking of integrin α4β1 or α4β7 showed no effect (Figure 3A). We then examined whether integrin α9β1-positive CRC cells were located in the perivascular regions in human CRC tissues. Immunofluorescent stainings for CD31 (EC marker) and integrin α9β1 were carried out in human primary colon cancer specimens. Integrin α9β1$^+$ CRC cells were expectedly found to locate in proximity to CD31$^+$ ECs (Figure 3B). Cumulatively, these findings suggest that EC-secreted EDA may interact with integrin α9β1 on neighboring CRC cells and therefore promote their metastasis.

We and others have demonstrated previously that colorectal cancer cells produce EDA to promote their tumorigenic and metastatic capacity acting in a paracrine fashion through binding to integrin α9β1 in neighboring CRC cells (14,15), we then performed immunoprecipitation assay to identify the interaction between EC-secreted EDA and integrin α9β1 on CRC cells. As shown in Figure 3C, immunoprecipitable integrin α9β1 was significantly reduced in CRC cells treated with CM from EDA-silenced ECs, indicating the existence of EDA and integrin α9β1 interactions in these cells.

To further determine if integrin α9β1 is critically required to mediate EC-secreted EDA effect, we stably overexpressed EDA in

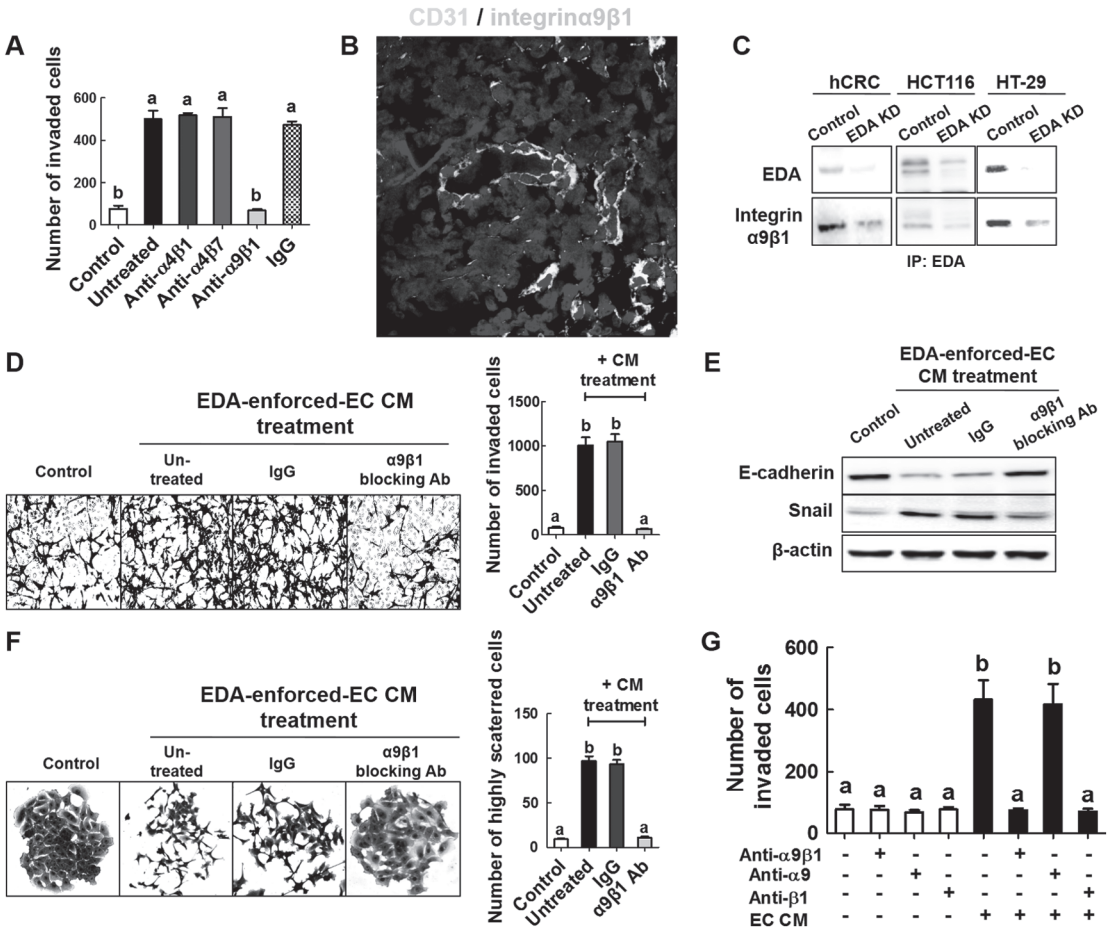

Fig. 3. Integrin α9β1 is the mediator for the effect of EC-secreted EDA on CRC cells. (**A**) Statistical analysis of the number of invaded EC CM-pretreated CRC cells in the presence of different integrin-blocking antibodies. (**B**) Immunofluorescence histochemistry of CRC specimens demonstrating integrin α9β1 positive CRC cell localization in the niche of ECs (CD31 positive). (**C**) Coimmunoprecipitation assay showing interactions of EDA with integrin α9β1 in EC CM-pretreated primary CRC cells (hCRC), colon cancer cell line HCT116 and HT-29. (**D**) Transwell assays of the invasion ability of control or EDA enforced EC CM-pretreated primary CRC cells with or without integrin α9β1-blocking antibody treatment (25 μg/ml). (**E**) Western blots of E-cadherin and Snail expression in control or EDA-enforced EC CM-pretreated primary CRC cells in the presence of or without integrin α9β1-blocking antibody treatment (25 μg/ml). (**F**) Crystal violet staining of the morphology change of control or EDA-enforced EC CM-pretreated primary CRC cells with or without integrin α9β1-blocking antibody treatment (25 μg/ml), and the statistical analysis of scattered cells in each group as shown ($P < 0.001$). (**G**) Transwell assays of the invasion ability of control or EDA-enforced EC CM-pretreated primary CRC cells in the presence of integrin α9β1 (25 μg/ml), integrin α9 (25 μg/ml) or integrin β1 (25 μg/ml)-blocking antibody treatment. Statistical analysis was done using one-way analysis of variance, and different letters associated with individual bars represent significant statistical differences among the groups ($P < 0.001$).

HUVECs in order to amplify the interaction between EDA and integrin α9β1. Strikingly, blocking of integrin α9β1 function substantially reversed the effect of CM of EDA-enforced HUVECs on CRC cells. Integrin α9β1-blocking antibody treatment reduced the invaded cells by ~90%, when compared with isotype control antibody treatment, which did not significantly alter the invasion capacity of EC CM cultured cells relative to untreated group (Figure 3D). Furthermore, integrin α9β1-blocking antibody treatment normalized the expressions of E-cadherin and Snail in EC CM-treated CRC cells (Figure 3E) and also dramatically reversed the morphology change of these cells (Figure 3F). To investigate which subunit of integrin α9β1 plays the predominant role in mediating the effect of EC CM on CRC cells, CRC cells were preincubated with antibody against α9β1, antibodies against the α9 or β1 subunit in the presence or absence of EC CM for 2 days, and then the invasion capacity of these cells were determined. Pre-incubation with anti-α9-blocking antibody did not exert retrieval effects on cell invasion, whereas pretreatment with anti-β1 integrin antibody neutralized the inducement of EC CM (Figure 3G) to CRC cells. All the evidence suggest that the effect of EC-derived EDA on CRC cells was mediated by integrin α9β1, especially by β1 subunit.

FAK signaling and Rac1 activation are required for EDA-mediated EMT and invasion

To explore the underlying molecular mechanism of the effect induced by EC-derived EDA, we screened several downstream signaling molecules of integrin and found that phosphorylations of extracellular signal-regulated kinase (ERK), Akt and FAK at Tyr397 were significantly increased in EC CM-treated CRC cells compared with the control cells (Figure 4A). In addition, phosphorylation of c-Src at Tyr416 was also increased in the presence of EC CM treatment (Figure 4A). Intriguingly, activity of the small GTPase Rac1, which induces

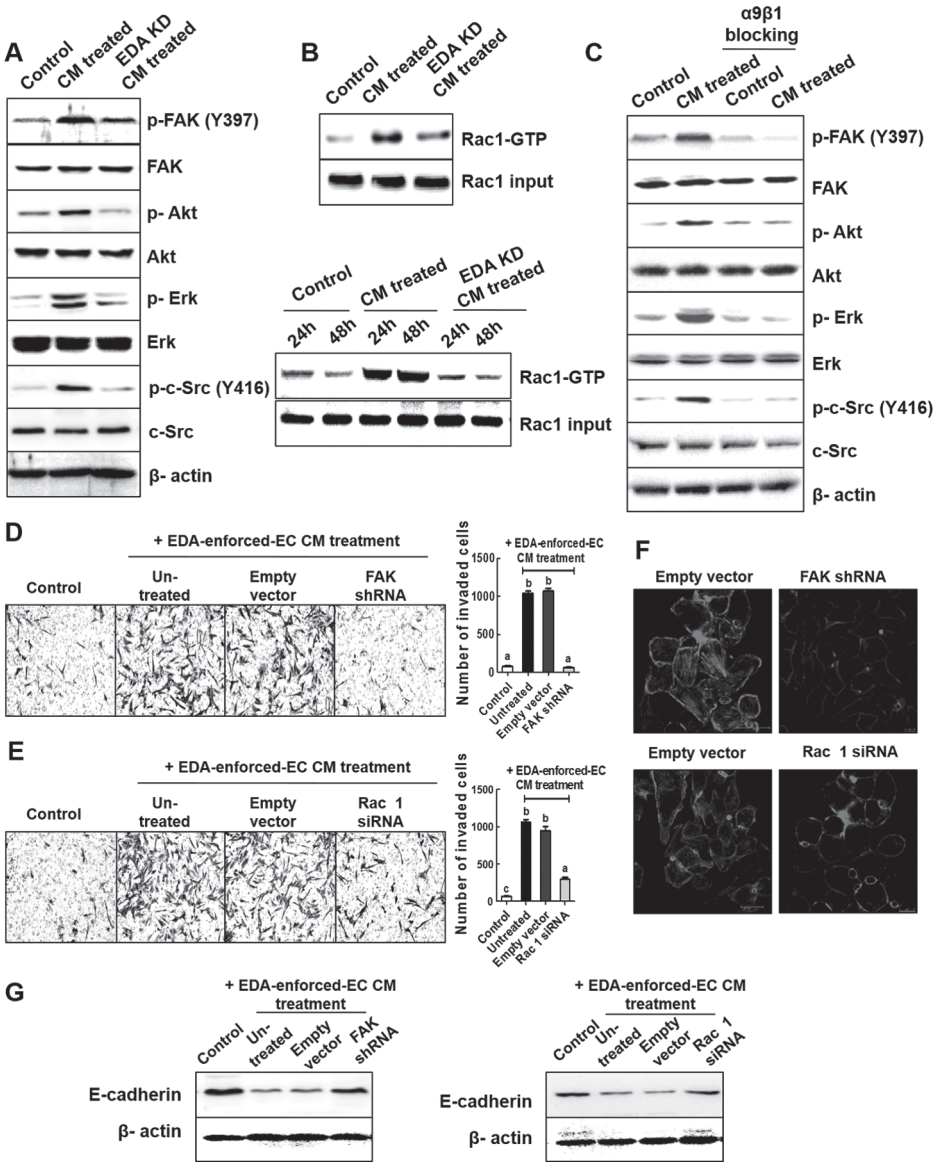

Fig. 4. FAK/ERK/Src/Rac pathway is involved in EDA–integrin α9β1 signal transduction. (**A**) Western blots of total as well as phosphorylated FAK, Akt, ERK1/2 and Src in control primary CRC cells and the primary CRC cells pretreated with EC CM or EDA knockdown (KD) EC CM. (**B**) Whole-cell lysates were used for Rac1 assay and immunoblotting. (**C**) Western blots of total as well as phosphorylated FAK, Akt, ERK1/2 and Src in control primary CRC cells and the primary CRC cells pretreated with EC CM with or without integrin α9β1-blocking treatment. (**D**) Transwell assay of control and FAK KD primary CRC cells in the presence of EDA-enforced EC CM treatment. (**E**) Transwell assay of control and Rac1 KD primary CRC cells in the presence of EDA-enforced EC CM treatment. (**F**) Immunofluorescent staining of F-actin of control, FAK KD (FAK shRNA) and Rac1 KD (Rac 1 siRNA) primary CRC cells in the presence of EDA-enforced EC CM treatment. (**G**) Western blots of E-cadherin of control, FAK KD (FAK shRNA) and Rac1 KD (Rac 1 siRNA) primary CRC cells in the presence of EDA-enforced EC CM treatment.

lamellipodia formation and motility (22–24), also increased in EC CM-treated CRC cells (Figure 4B). Expectedly, EC CM-mediated increase of phosphorylations of FAK, ERK and c-Src was reversed by integrin α9β1-blocking treatment (Figure 4C). Since FAK is a downstream mediator of integrin signaling (25), and plays an important role in promoting CRC pathogenesis (18,26), to determine the role of FAK signaling and Rac1 activation in EDA-mediated invasion and EMT, we transiently transfected CRC cells with a plasmid expressing FAK shRNA or Rac1 siRNA that can efficiently silence FAK or Rac1 in CRC cells. Even in the presence of CM from EDA overexpressing ECs, FAK shRNA still drastically reversed the induced invasion of CM-treated CRC cells (Figure 4D). In contrast, Rac1 siRNA moderately normalized the invasion capacity of EC CM-treated CRC cells (Figure 4E). The rescue effect of FAK shRNA on cell invasion was dramatically greater than that of Rac1 siRNA, suggesting that FAK may be more specifically required for the effect of EC-derived EDA on CRC cells. Furthermore, the formation of stress fibers in CRC cells, which were induced by EC-secreted EDA, was diminished by FAK shRNA or Rac1 siRNA (Figure 4F). Finally, the downregulation of E-cadherin was also rescued by FAK shRNA or Rac1 siRNA (Figure 4G). These results suggest that FAK signaling and Rac1 activation are required for EDA-mediated invasion, morphological changes and EMT.

Role of different signaling pathways in EDA-mediated EMT and invasion

To determine the relative contribution of different signaling in EC-secreted EDA facilitated EMT and invasion of CRC cells. CRC cells were pretreated with CM from EDA-enforced ECs and were treated with the following pharmacological inhibitors for 48 h before analyzing them by immunocytochemistry, invasion assay and immunoblotting: dimethyl sulfoxide (vehicle), PD098059 (a specific MEK inhibitor), LY294002 (specific PI3K inhibitors) and PP1 (a specific c-Src family kinase inhibitor). Inhibition of MEK/ERK or c-Src efficiently suppressed stress fiber formation and invasion characteristics of EMT but did not substantially affect cell viability, whereas inhibition of PI3K had no effect (Figure 5A–C). Furthermore, only the inhibition of MEK/ERK reversed the suppression of E-cadherin (Figure 5D). On the other hand, inhibitors of c-Src did not substantially inhibit phosphorylation of Akt, whereas phosphorylation of ERK was efficiently inhibited (Figure 5D). Expectedly, inhibition of MEK/ERK or c-Src also significantly reduced EC CM-induced cell

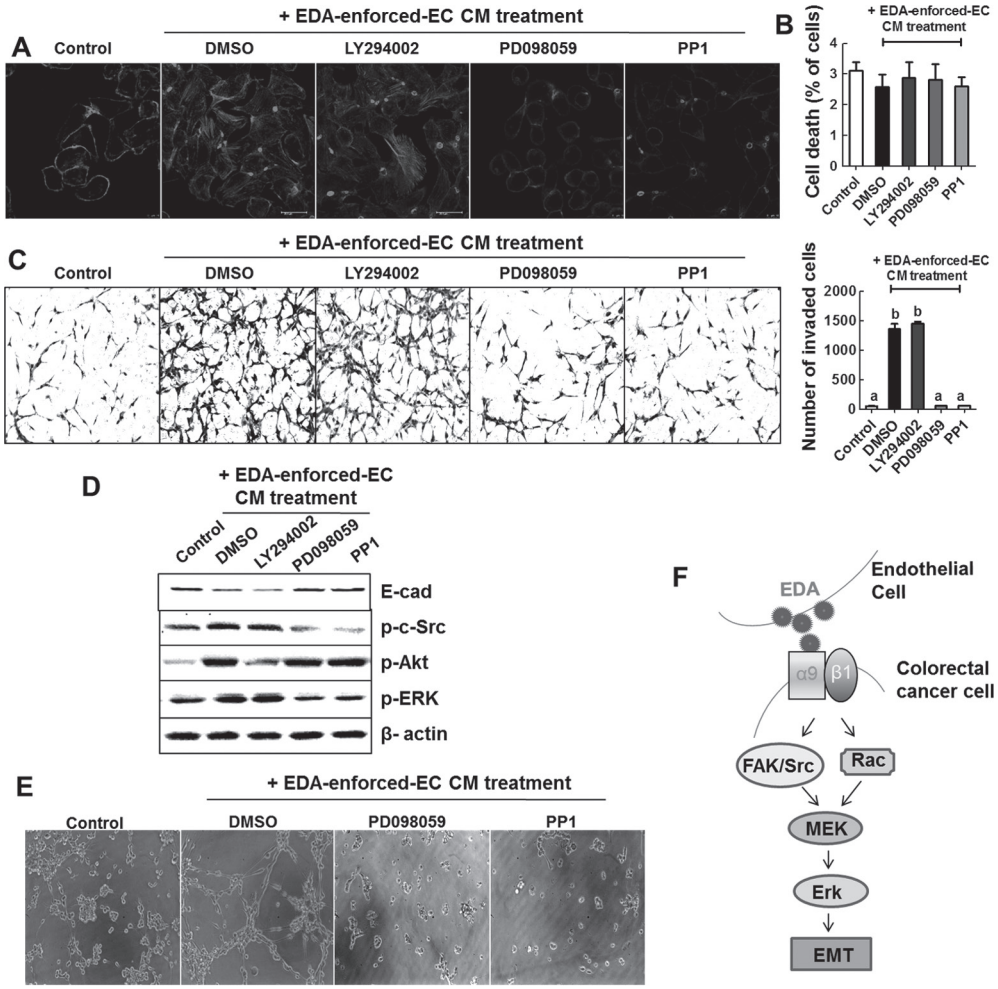

Fig. 5. Erk signaling critically mediates the effect of EC-derived EDA on CRC cells. (**A**) Immunofluorescent staining of F-actin of control and EDA-enforced EC CM-pretreated primary CRC cells in the presence of dimethyl sulfoxide (DMSO, vehicle), PD098059 (a specific MEK inhibitor, 25 μM), LY294002 (specific PI3K inhibitor, 25 μM) and PP1 (a specific c-Src family kinase inhibitor, 25 μM). (**B**) Cell viability assay of control and EDA-enforced EC CM-pretreated primary CRC cells in the presence of DMSO, PD098059, LY294002 and PP1. (**C**) Transwell assay of control and EDA-enforced EC CM-pretreated primary CRC cells in the presence of DMSO, PD098059, LY294002 and PP1. Statistical analysis was done using one-way analysis of variance,and different letters associated with individual bars represent significant statistical differences among the groups ($P < 0.001$). (**D**) Western blots of E-cadherin, phosphorylated Akt, ERK1/2 and Src of control and EDA-enforced EC CM-pretreated primary CRC cells in the presence of DMSO, PD098059, LY294002 and PP1. (**E**) Adhesion ability assay of control and EDA-enforced EC CM-pretreated primary CRC cells in the presence of DMSO, PD098059, LY294002 and PP1. (**F**) Proposed EDA–integrin α9β1 interaction signaling pathway between ECs and CRC cells.

adhesion of CRC cells (Figure 5E). These results indicate that c-Src/ERK signaling, in addition to FAK signaling, is critically involved in mediating EC-secreted EDA-induced EMT, cell invasion and down-regulation of E-cadherin in CRC cells, whereas PI3K is not critically required for these effect. Based on these observations, we proposed a signaling pathway for EC-secreted EDA regulation of CRC cell EMT (Figure 5F).

The level of EC-secreted EDA and expression of integrin α9β1 correlate with E-cadherin expression and also stage progression in human CRCs

We have demonstrated in our previous study that EDA level in the serum or in the tumor tissue of advanced stage CRC patients is significantly higher than that of early stage patients (14). To further determine whether EC-secreted EDA is correlated with E-cadherin expression in human CRCs via an integrin α9β1-dependent manner, we measured the secreted EDA level in isolated ECs from CRC surgical specimens and also determined the expression of integrin α9β1 of the same tumor tissue. Expectedly, we found that the secreted EDA level in isolated ECs was positively correlated to the expression of integrin α9β1 of the same tumor tissue (Figure 6A). Of note, significant difference for the secreted EDA level in isolated ECs and integrin α9β1 expression of the same tumor tissue was observed between early (stage I–II) and metastatic advanced (stages III–IV) CRCs (Figure 6B), whereas difference between early (stage I) and non-metastatic advanced (stage II) cancer showed no statistical significance (Figure 6B). The isolated ECs from CRC patients with recurrence after surgical resection exhibited significantly higher secreted EDA level accompanied with higher integrin α9β1 expression level in the same CRCs relative to those with no recurrence (Figure 6C). Next, the expression of integrin α9β1 and E-cadherin was immunohistochemically analyzed in serially sectioned 63 human CRC tissues from stages I, II, III to IV CRC patients (Figure 6D). Furthermore, statistical analysis showed an inverse correlation between integrin α9β1 and E-cadherin expression (Figure 6E). These observations indicate that EC-secreted EDA plays a oncogenic role in facilitating the progression of CRCs from non-invasive to invasive malignancies through activating an integrin α9β1-mediated EMT.

Discussion

We and others have demonstrated that CRC cell-derived EDA plays a critical role in promoting tumor vasculogenesis, tumorigenesis and metastasis (10–15). In our current studies, however, we defined a previously unrecognized mechanism through which ECs activate EMT signaling to promote CRC cell metastasis—namely, production of the soluble EDA ligand. Changes in the stromal cells appropriate to support the growth of the tumor have been reported, and several previous studies have indicated that ECs play a more active role in regulating tumor cell behaviors than simply providing the physical structure that forms conduits for blood flow (7–10). We found that HUVEC CM promotes the invasion of hCRC cells 6-fold in comparison with control CM. This intriguing phenomenon may be explained by two aspects. One is that even the normal ECs may secret oncogenic factors to sustain CRC cell survival and metastatic capacity, and another is that CRC cells express abundant and active receptors addicted to the oncogenic factors (e.g. EDA) secreted by ECs.

In this study, we mechanistically identified integrin α9β1 as the predominant receptor addicted to EC-secreted EDA, and integrin α9β1

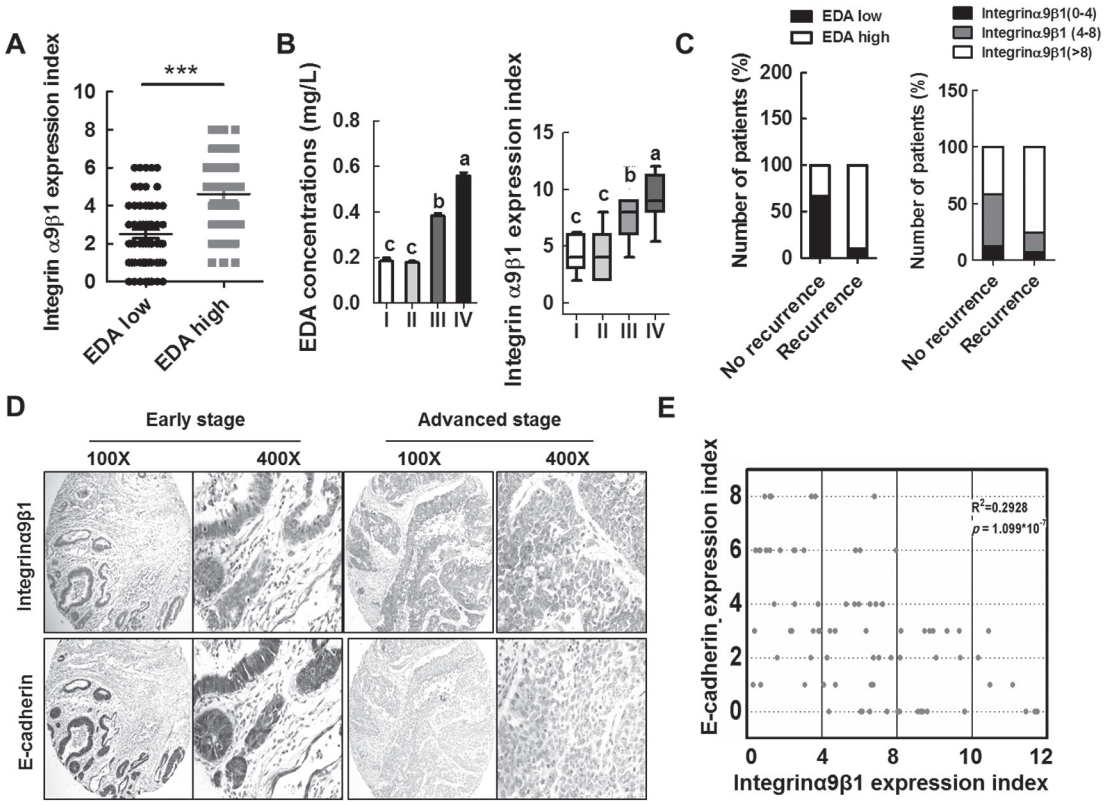

Fig. 6. EC-derived EDA and integrin α9β1 level is correlated with clinicopathological features in CRCs. (**A**) Statistical analysis (Student's *t*-test) of the correlation between integrin α9β1 expression in the CRC tumor tissue and the secreted EDA level of isolated EC from the same tumor tissue ($n = 98$). ***$P < 0.0001$. (**B**) Statistical analysis of EC-derived EDA level and integrin α9β1 expression in the CRC tumor tissue among CRCs of different stages (one-way analysis of variance) (I , $n = 18$; II, $n = 117$; III, $n = 83$; IV, $n = 34$). $P < 0.01$. (**C**) Statistical analysis (Fisher's exact test) of the correlation between EC-derived EDA level and integrin α9β1 expression in the CRC tumor tissue and the risk of recurrence in stage I, II and III CRC patients ($n = 57$ for No recurrence; $n = 41$ for Recurrence; $P = 0.004$ between No recurrence and Recurrence). (**D** and **E**) Immunostaining (D) of, and statistical analysis (E) of the correlation between, integrin α9β1 expression level and the expression level of E-cadherin in human CRC tissues ($n = 81$). $P < 0.001$ (Spearman's correlation).

signaling as a molecular basis by which EC-derived EDA induces signaling transduction, EMT and invasion of CRC cells. The observation that CSCs accumulate in perivascular regions has been reported by several studies (6,7), and EMT is critically associated with CSC characteristics. We have revealed previously that integrin α9β1-positive CRC cells are a subpopulation with striking stemness characteristics (14). In this study, integrin α9β1-positive CRC cells were found to reside in perivascular niches in CRCs, indicating that EC-secreted EDA may be a potent chemokine to recruit integrin α9β1-positive cells into the perivascular niche and further reeducate these cells to acquire an EMT phenotype and therefore promote their invasion capacity. Our findings also reveal a novel mechanism through which the CSC population is enriched in the perivascular regions.

We provide several lines of evidence demonstrating that EC-secreted EDA promotes EMT phenotype in neighboring CRC cells via interacting with integrin α9β1 to activate FAK as well as Rac signalings. Integrins can alter cellular behavior through the recruitment and activation of signaling proteins such as non-receptor tyrosine kinases including FAK and c-Src that form a dual kinase complex. The FAK–Src complex binds to and can phosphorylate various adaptor proteins such as p130Cas and paxillin. In normal cells, multiple integrin-regulated linkages exist to activate FAK or Src. Activated FAK–Src functions to promote cell motility, cell cycle progression and cell survival. Recent studies have found that the FAK–Src complex is activated in many tumor cells and generates signals leading to tumor growth and metastasis. Our study showed that EC-derived EDA is a critical trigger to the activation of FAK, Src, Rac, Akt and Erk presumably via regulation of integrin expression and/or cooperation with integrins. EC CM was demonstrated to potently upregulate integrin α9β1 expression in CRC cells, and a binding of EDA and integrin α9β1 was also confirmed under coimmunoprecipitation conditions. Therefore, it is possible that EDA regulates integrin α9β1 induction and thus regulates its signaling transduction activity. To our knowledge, this study showed for the first time that EC-derived EDA can regulate specific CRC integrin expression and its subsequent signaling transduction, leading to EMT and invasion of CRCs. It is worth exploring by which precise mechanism EDA can modulate integrin α9β1 expression.

We observed that the mRNA as well as protein level of E-cadherin was substantially reduced, whereas the levels of Snail and vimentin in EC CM-treated CRC cells were robustly increased, which suggest that EC-secreted EDA may initiate the regulation of these proteins at the mRNA level, but the precise mechanism need to be further revealed. Reconstitution of E-cadherin results in a tumor cell reversion from an invasive mesenchymal phenotype to a benign epithelial phenotype (27–29). On the other hand, suppression of high endogenous E-cadherin expression renders non-invasive cells partially invasive (27,29). Although it has been found that downregulation of E-cadherin was not the only contributor to EDA-mediated phenotypes. In the future, it will be important to elucidate whether the induction of specific mesenchymal markers (e.g. integrin) (30–32), in addition to the downregulation of tumor suppressors such as E-cadherin, is required for full invasiveness during progression of colon cancer.

Rac1 activity was demonstrated to be significantly enhanced by EC CM treatment, and previous studies have also implicated Rac1 as one of the key signaling components controlling actin cytoskeleton organization in mammalian cells (23). The molecular mechanism underlying Rac1-mediated cell migration, invasion and adhesion has been a subject of intensive studies. Although it is well documented that Rac1 can regulate PI3K/AKT as well as Erk kinase signalings, the definitive causal relationship between Rac1 activity and the adhesion contact components such as FAK and Src remains elusive. In our current study, we have demonstrated that the rescue effect of FAK suppression to EC-derived EDA-induced EMT in CRC cells is more efficient than Rac1 interruption, suggesting that Rac1 activation is just a part of pathway in EC-derived EDA-induced effect, and Rac1 may be a downstream factor of FAK in this event.

In summary, our study defines a mechanism for the oncogenic significance of ECs that leads to integrin/FAK/Rac1 activation in CRC cells that, in turn, promotes their EMT phenotype and metastatic capacity. Our present findings in the field of EC-derived EDA have opened up a new understanding of how ECs contribute to cancer pathogenesis.

Supplementary material

Supplementary Materials can be found at http://carcin.oxfordjournals.org/

Funding

National Natural Science Foundation of China (81370063 to J.O., 30973430, 81272364 to H.L.).

Acknowledgements

We thank Wei Sun of the Central Laboratory of Third Military Medical University for her excellent technical assistance in confocal laser scanning microscopy, and Feng Wu and Qiang Wang for their help in evaluation for the results of immunohistochemistry. *Ethics approval*: All studies involved in human samples were approved by Southwest Hospital and informed consent obtained from each participant. All animal studies were approved by the Animal Care and Use Committee of the Third Military Medical University, Chongqing, China.

Conflict of Interest Statement: None declared.

References

1. Zeng,Q. *et al.* (2005) Crosstalk between tumor and endothelial cells promotes tumor angiogenesis by MAPK activation of Notch signaling. *Cancer Cell*, **8**, 13–23.
2. Andrade,S.P. *et al.* (1992) Effects of tumour cells on angiogenesis and vasoconstrictor responses in sponge implants in mice. *Br. J. Cancer*, **66**, 821–826.
3. Li,D. *et al.* (1994) The observation of angiogenin and basic fibroblast growth factor gene expression in human colonic adenocarcinomas, gastric adenocarcinomas, and hepatocellular carcinomas. *J. Pathol*., **172**, 171–175.
4. Takahashi,Y. *et al.* (1995) Expression of vascular endothelial growth factor and its receptor, KDR, correlates with vascularity, metastasis, and proliferation of human colon cancer. *Cancer Res*., **55**, 3964–3968.
5. Weidner,N. *et al.* (1991) Tumor angiogenesis and metastasis–correlation in invasive breast carcinoma. *N. Engl. J. Med*., **324**, 1–8.
6. Butler,J.M. *et al.* (2010) Instructive role of the vascular niche in promoting tumour growth and tissue repair by angiocrine factors. *Nat. Rev. Cancer*, **10**, 138–146.
7. Butler,J.M. *et al.* (2010) Endothelial cells are essential for the self-renewal and repopulation of Notch-dependent hematopoietic stem cells. *Cell Stem Cell*, **6**, 251–264.
8. Krishnamurthy,S. *et al.* (2010) Endothelial cell-initiated signaling promotes the survival and self-renewal of cancer stem cells. *Cancer Res*., **70**, 9969–9978.
9. Galan-Moya,E.M. *et al.* (2011) Secreted factors from brain endothelial cells maintain glioblastoma stem-like cell expansion through the mTOR pathway. *EMBO Rep*., **12**, 470–476.
10. Rybak,J.N. *et al.* (2007) The extra-domain A of fibronectin is a vascular marker of solid tumors and metastases. *Cancer Res*., **67**, 10948–10957.
11. Ou,J.J. *et al.* (2010) Colorectal tumor derived fibronectin alternatively spliced EDA domain exserts lymphangiogenic effect on human lymphatic endothelial cells. *Cancer Biol. Ther*., **9**, 186–191.
12. Ou,J. *et al.* (2011) Endostatin suppresses colorectal tumor-induced lymphangiogenesis by inhibiting expression of fibronectin extra domain A and integrin α9. *J. Cell. Biochem*., **112**, 2106–2114.
13. Xiang,L. *et al.* (2012) The extra domain A of fibronectin increases VEGF-C expression in colorectal carcinoma involving the PI3K/AKT signaling pathway. *PLoS One*, **7**, e35378.
14. Ou,J. *et al.* (2013) Fibronectin extra domain A (EDA) sustains CD133(+)/CD44(+) subpopulation of colorectal cancer cells. *Stem Cell Res*., **11**, 820–833.
15. Sun,X. *et al.* (2014) The EDA-containing cellular fibronectin induces epithelial-mesenchymal transition in lung cancer cells through integrin

α9β1-mediated activation of PI3-K/AKT and Erk1/2. *Carcinogenesis*, **35**, 184–191.
16. Shinde,A.V. *et al.* (2008) Identification of the peptide sequences within the EIIIA (EDA) segment of fibronectin that mediate integrin alpha9beta1-dependent cellular activities. *J. Biol. Chem.*, **283**, 2858–2870.
17. Allen,M.D. *et al.* (2011) Clinical and functional significance of α9β1 integrin expression in breast cancer: a novel cell-surface marker of the basal phenotype that promotes tumour cell invasion. *J. Pathol.*, **223**, 646–658.
18. Chen,Y. *et al.* (2010) The effect of focal adhesion kinase gene silencing on 5-fluorouracil chemosensitivity involves an Akt/NF-kappaB signaling pathway in colorectal carcinomas. *Int. J. Cancer*, **127**, 195–206.
19. Kim,H.P. *et al.* (2005) TGF-beta1-mediated activations of c-Src and Rac1modulate levels of cyclins and p27(Kip1) CDK inhibitor in hepatoma cells replated on fibronectin. *Biochim. Biophys. Acta*, **1743**, 151–161.
20. Brand,M.I. *et al.* (1996) Development of a reliable colorectal cancer liver metastasis model. *J. Surg. Res.*, **63**, 425–432.
21. Liao,Y.F. *et al.* (2002) The EIIIA segment of fibronectin is a ligand for integrins alpha 9beta 1 and alpha 4beta 1 providing a novel mechanism for regulating cell adhesion by alternative splicing. *J. Biol. Chem.*, **277**, 14467–14474.
22. Machesky,L.M. *et al.* (1996) Rho: a connection between membrane receptor signalling and the cytoskeleton. *Trends Cell Biol.*, **6**, 304–310.
23. Guo,F. *et al.* (2006) Genetic deletion of Rac1 GTPase reveals its critical role in actin stress fiber formation and focal adhesion complex assembly. *J. Biol. Chem.*, **281**, 18652–18659.
24. Hall,A. (1998) Rho GTPases and the actin cytoskeleton. *Science*, **279**, 509–514.
25. Mitra,S.K. *et al.* (2005) Focal adhesion kinase: in command and control of cell motility. *Nat. Rev. Mol. Cell Biol.*, **6**, 56–68.
26. Lee,S.H. *et al.* (2011) Role of hypoxia-induced fibronectin-integrin β1 expression in embryonic stem cell proliferation and migration: involvement of PI3K/Akt and FAK. *J. Cell. Physiol.*, **226**, 484–493.
27. Lu,Z. *et al.* (2003) Downregulation of caveolin-1 function by EGF leads to the loss of E-cadherin, increased transcriptional activity of beta-catenin, and enhanced tumor cell invasion. *Cancer Cell*, **4**, 499–515.
28. Derksen,P.W. *et al.* (2006) Somatic inactivation of E-cadherin and p53 in mice leads to metastatic lobular mammary carcinoma through induction of anoikis resistance and angiogenesis. *Cancer Cell*, **10**, 437–449.
29. Arima,Y. *et al.* (2008) Rb depletion results in deregulation of E-cadherin and induction of cellular phenotypic changes that are characteristic of the epithelial-to-mesenchymal transition. *Cancer Res.*, **68**, 5104–5112.
30. Cabodi,S. *et al.* (2010) Integrin signalling adaptors: not only figurants in the cancer story. *Nat. Rev. Cancer*, **10**, 858–870.
31. Ginestier,C. *et al.* (2010) CXCR1 blockade selectively targets human breast cancer stem cells in vitro and in xenografts. *J. Clin. Invest.*, **120**, 485–497.
32. Hur,K. *et al.* (2013) MicroRNA-200c modulates epithelial-to-mesenchymal transition (EMT) in human colorectal cancer metastasis. *Gut*, **62**, 1315–1326.

Received August 29, 2013; revised March 12, 2014; accepted March 19, 2014